Numerical Simulation of Volcanic Jets

Marica Pelanti and Randall J. LeVeque

Abstract. We numerically model the dynamics of explosive volcanic eruptions to study the fluid-dynamic structure of jets that develop in such processes. The eruptive mixture is described as a two-phase flow made of gas and solid particles. The hyperbolic portion of these equations consists of the compressible Euler equations for the gas phase and the non-strictly hyperbolic conservation laws for a pressureless dust, used to model the solid phase. These equations are coupled together through terms modeling inter-phase drag and heat transfer. Gravity is also taken into account for both phases. Ejection velocities in eruptions are often large enough that the jet is supersonic relative to the mixture sound speed, leading to the development of internal shock wave structures. We solve the system of equations by employing a high-resolution finite volume method based on wave propagation algorithms.

1. Introduction

Explosive volcanic events are characterized by the injection into the atmosphere of a mixture of gas and pyroclastic material at high velocity and temperature. Extensive work has been made since the mid-1980s on the numerical modeling of such phenomena, e.g. [2, 10, 11, 19, 20], which has shown how numerical simulation is an important tool for better understanding the complex and highly nonlinear thermo-fluid dynamic mechanisms governing these processes.

Here our aim is to numerically model the dynamics of explosive volcanic eruptions by employing a finite volume method based on the wave propagation algorithms described in [5]. In particular, we are interested in studying the fluid dynamic structure of the jet thrust region that characterizes overpressured supersonic eruptive flows. Gases containing particulate material can have very low sound speed, so that volcanic jets are often supersonic, and may develop complex shock wave patterns [4] above the conduit exit.

In Section 2 we illustrate the physical model that we employ to describe the eruptive mixture, while the numerical method used is presented in Section 3. Results of our computations are reported in Section 4.

2. Physical Model

Our physical model follows existing work on the computation of two-phase flows [3, 17, 18] and the simulation of volcanic processes [2, 10, 11, 19]. The eruptive mixture is modeled as a two-phase flow composed of solid particles (dust) suspended in a gaseous phase. Each phase is considered as a continuum described by macroscopic quantities, with the gas phase being compressible, and the solid phase incompressible at a microscopic level (microscopic density ρ_d = constant). Moreover, we assume that the dust phase is dilute (dust volume fraction $\vartheta_d \ll 1$), and has negligible inter-particle interaction, so that it will be considered *pressureless*. The governing equations consist of the compressible Euler equations for the gas coupled with conservation laws for the dust phase through terms modeling interphase drag and heat transfer. Gravity is also take into account for both phases. We neglect other physical effects such as gas viscosity, turbulence, and water vapor content. This is a reasonable assumptions in the specific small-time scale explosive volcanic processes we are interested in.

In the following, subscripts g and d refer to the gas and dust phase, respectively, and part of the nomenclature used is summarized in Table 1. The equations expressing the conservation of mass, momentum and total energy for the two phases are:

$$\frac{\partial \rho}{\partial t} + \nabla \cdot (\rho \mathcal{V}_g) = 0\,, \tag{1a}$$

$$\frac{\partial}{\partial t}(\rho \mathcal{V}_g) + \nabla \cdot (\rho \mathcal{V}_g \otimes \mathcal{V}_g + pI) = \rho \mathfrak{g} - D(\mathcal{V}_g - \mathcal{V}_d)\,, \tag{1b}$$

$$\frac{\partial E}{\partial t} + \nabla \cdot ((E+p)\mathcal{V}_g) = \rho \mathcal{V}_g \cdot \mathfrak{g} - D(\mathcal{V}_g - \mathcal{V}_d) \cdot \mathcal{V}_d - \mathcal{Q}(T_g - T_d)\,, \tag{1c}$$

$$\frac{\partial \beta}{\partial t} + \nabla \cdot (\beta \mathcal{V}_d) = 0\,, \tag{1d}$$

$$\frac{\partial}{\partial t}(\beta \mathcal{V}_d) + \nabla \cdot (\beta \mathcal{V}_d \otimes \mathcal{V}_d) = \beta \mathfrak{g} + D(\mathcal{V}_g - \mathcal{V}_d)\,, \tag{1e}$$

$$\frac{\partial \Omega}{\partial t} + \nabla \cdot (\Omega \mathcal{V}_d) = \beta \mathcal{V}_d \cdot \mathfrak{g} + D(\mathcal{V}_g - \mathcal{V}_d) \cdot \mathcal{V}_d + \mathcal{Q}(T_g - T_d)\,. \tag{1f}$$

The gaseous phase is assumed to follow the ideal polytropic gas thermodynamic relations $p_g = (\gamma - 1)\rho_g \varepsilon_g$ and $\varepsilon_g = c_{vg} T_g$, γ, c_{vg} = constant. The energy equation for the dust phase is $\varepsilon_d = c_{vd} T_d$, c_{vd} = constant. The drag function has the form

$$D = \frac{3}{4} C_{\mathrm{d}} \frac{\beta \rho}{\rho_d d} |\mathcal{V}_g - \mathcal{V}_d|\,, \tag{2}$$

where d is the dust particle diameter, and C_{d} the drag coefficient, which we take as [10, 11]

$$C_{\mathrm{d}} = \begin{cases} \frac{24}{Re}\left(1 + 0.15 Re^{0.687}\right) & \text{if } Re < 1000\,, \\ 0.44 & \text{if } Re \geq 1000\,. \end{cases} \tag{3}$$

Above $Re = \rho\, d|\mathcal{V}_g - \mathcal{V}_d|/\mu$ is the Reynolds number, with μ denoting the dynamic viscosity of the gas. The heat transfer function is given by

$$\mathcal{Q} = \frac{Nu\, 6\kappa_g \beta}{\rho_d d^2}\,, \tag{4}$$

where Nu is the Nusselt number, which we express as $Nu = 2 + 0.65 Re^{1/2} Pr^{1/3}$. Here $Pr = c_{pg}\mu/\kappa_g$ is the Prandtl number, κ_g denotes the gas thermal conductivity, and c_{pg} the gas specific heat at constant pressure.

ϑ_g, ϑ_d = volume fractions, $\vartheta_g + \vartheta_d = 1$, $\vartheta_d \ll 1$;
ρ_g, ρ_d = material microscopic mass densities (ρ_d = constant);
$\rho = \vartheta_g \rho_g$ = gas macroscopic density;
$\beta = \vartheta_d \rho_d$ = dust macroscopic density (concentration);
p_g = gas pressure, $p = \vartheta_g p_g$;
$\mathcal{V}_g = (u_g, v_g, w_g)^{\mathrm{T}}$, $\mathcal{V}_d = (u_d, v_d, w_d)^{\mathrm{T}}$ = vectorial velocities;
ε_g, ε_d = specific internal energies;
$e_g = \varepsilon_g + \frac{1}{2}\|\mathcal{V}_g\|^2$, $e_d = \varepsilon_d + \frac{1}{2}\|\mathcal{V}_d\|^2$ = specific total energies;
$E = \vartheta_g \rho_g e_g$, $\Omega = \vartheta_d \rho_d e_d$ = total energies per unit volume;
T_g, T_d = temperatures;
c_{pg}, c_{vg}; c_{vd} = specific heats ($\gamma = c_{pg}/c_{vg}$);
$\mathfrak{g} = (0, 0, -g)^{\mathrm{T}}$ = gravity acceleration (z direction).

TABLE 1. Nomenclature.

3. Numerical Method

We solve the system (1) by employing a fractional step technique, in which we alternate between a time step on the homogeneous hyperbolic system and a time step on a system of ODEs for the source terms, with the exception of the gas gravity term, which is incorporated in the left hand side of the equations. To solve the homogeneous hyperbolic portion of the system we use the wave propagation algorithms [5] as implemented in the CLAWPACK software [6]. These are a high-resolution finite volume methods based on solving Riemann problems at each cell interface at every time step. In particular, we adopt the *f-wave* formulation [1] of the algorithm, in which the flux difference $f(Q^{\mathrm{R}}) - f(Q^{\mathrm{L}})$ between neighboring cells with data Q^{R} and Q^{L} is decomposed into waves (f-waves) that are then used to update the cell averages. Second-order correction terms and limiters are applied to these f-waves.

Notice that coupling between the two phases takes place only through drag and heat transfer terms, so that the hyperbolic homogeneous equations decouple into two separate systems for the gas and dust phase. Therefore, we can solve the two sets of equations separately.

The gas phase equations are the standard Euler equations of gas dynamics for an ideal gas, and for their numerical approximation we employ the Roe linearization [16]. In particular, following the method presented in [8], we incorporate the effect of the gas gravity source term into the Riemann solution, so that we decompose in f-waves the sum of the gas flux difference and the contribution of the source term as $f_g(Q_g^{\mathrm{R}}) - f_g(Q_g^{\mathrm{L}}) - \Psi = \sum_p \mathcal{Z}^p$, where each f-wave $\mathcal{Z}^p$ is taken as a scalar multiple of the pth Roe eigenvector $\hat{r}^p$, and has speed given by the pth Roe eigenvalue $\hat{\lambda}^p$. The gravity contribution Ψ arising from the gas gravity term ψ_g is defined as $\Psi = \Delta z(\psi_g^{\mathrm{L}} + \psi_g^{\mathrm{R}})/2$, where $\Delta z = z^{\mathrm{R}} - z^{\mathrm{L}}$ is the difference in the vertical coordinate of the centroids of the two cells adjacent to this interface. This formulation for gravity allows the accurate modeling of small perturbations from gravitational steady state, which is important in the applications considered here, where dusty gas jets enter an atmosphere in hydrostatic balance conditions.

The non-strictly hyperbolic equations of the pressureless dust phase are solved by employing the algorithm presented in [7]. With the f-wave formulation we generally use only a single wave with magnitude $\mathcal{Z} = f_d(Q_d^{\mathrm{R}}) - f_d(Q_d^{\mathrm{L}})$ and speed $\hat{u}_d$ defined as the usual Roe average for the dust velocity, based on the dust density. This can also be shown to be the correct delta-shock propagation speed in the pressureless equations [7]. The only time we use two waves is if $u_d^{\mathrm{L}} < 0 < u_d^{\mathrm{R}}$, in which case they are spreading with a vacuum state in between. Then we take $\mathcal{Z}^1 = -f_d(Q_d^{\mathrm{L}})$ and $\mathcal{Z}^2 = f_d(Q_d^{\mathrm{R}})$, with speeds $s^1 = u_d^{\mathrm{L}}$ and $s^2 = u_d^{\mathrm{R}}$, respectively.

The dust gravity source term, together with terms for inter-phase drag and heat exchange, is handled with a fractional step procedure, as already mentioned. A semi-analytical approach is used to treat drag and heat transfer, in which we exploit the structure of the exact solution of the systems of ODEs arising from these two contributions considered separately. This technique is efficient in modeling mechanical and thermal exchange for a wide range of relaxation time scales.

For a detailed description of the numerical method employed to solve the equations of the physical model (1), we refer to [9, 15].

4. Numerical Simulations

We consider the injection of a hot supersonic particle-laden gas from a volcanic vent into a cooler atmosphere (e.g. [2, 10, 12, 19]). Initially, a standard atmosphere vertically stratified in pressure and temperature is set all over the domain. At the vent, the gas pressure, the velocities and temperatures of the two phases, and the dust volumetric fraction are assumed to be fixed and constant. The ground boundary is modeled as a free-slip reflector. For two-dimensional experiments, an axisymmetric configuration of the flow is used, and system (1) is rewritten in cylindrical coordinates. We obtain a new set of equations with the same form of (1) on the left-hand side, but with an additional geometric source term on the right-hand side, which is treated numerically with an operator splitting technique. In this two-dimensional axisymmetric configuration, half of the volcanic vent, of

diameter D_v, is located in the lower left-hand corner of the computational domain, the symmetry axis is modeled as a free-slip reflector, while the upper and right-hand edges of the domain are free flow boundaries and all the variables gradients are set to zero. For three-dimensional experiments we have performed our simulations in an octant, see [15].

Computations are performed by using the basic Fortran 77 routines of the software CLAWPACK [6]. The adaptive mesh refinement version (AMRCLAW) is also being used for further experiments [15].

Several numerical experiments have been performed by using the model presented in Sections 2 and 3. A set of simulations has been focused on pyroclastic dispersion dynamics processes of pressure-balanced eruptions, following in particular the work in [10]. We refer to [15] for an illustration of the results obtained, which showed qualitative agreement with the cited work above.

Here we report selected results of another set of numerical experiments in which we have studied the decompression phase of underexpanded supersonic jets with different crater morphology, focusing on shock wave patterns that may develop in the jet thrust region. This is also part of a joint work with A. Neri and T. Esposti Ongaro (who made preliminary studies on the subject [13]), with the aim of comparing results obtained with our approach with those computed by using the numerical model of their Pyroclastic Dispersion Analysis Code (PDAC) [11].

Vent conditions are taken from [12, 14], and are summarized below, together with some physical parameters for the particulate phase

$v_{g,v}$ [m/s]	$v_{d,v}$ [m/s]	$p_{g,v}$ [MPa]	T_v [K]	$\vartheta_{d,v}$	$d\,[\mu\text{m}]$	$\rho_d\,[\text{kg/m}^3]$
211.0	201.0	4.6	1100	0.063	200	2360

The gas phase is considered dry air, and it has $R = 287\,\text{J/(kg K)}$ (gas constant), $\gamma = 1.4$, $\mu = 10^{-5}$ Pa s, and $\kappa_g = 0.05$ W/(m K). Moreover, for the dust $c_{vd} = 1.3 \times 10^3\,\text{J/(kg K)}$. The volcanic crater is modeled as a wedge with inner radius $D_v/2$, $D_v = 127$ m, and outer radius $R = 254$ m. We will present results for two different crater opening angle (with respect to the vertical): $\alpha = 90^\circ$ (no crater, free decompression) and $\alpha = 30^\circ$.

Figures 1 and 2 show contour plots of the dust density at different times as obtained for $\alpha = 90^\circ$ and $\alpha = 30^\circ$, respectively, on an uniform grid of 300×600 cells with cell size = 12.7 m. Common features to the two simulations are the rapid growth of the jet diameter above the vent and the unsteady vortical structure that characterizes the jet head, and which is caused by the initial rapid acceleration of the fluid.

In Figures 3 and 4 we display the pressure gradient for the two cases at $t = 4$ and 30 s. From these figures we can observe both atmospheric shocks waves propagating radially from the vent, and the development of shock patterns inside the jets. In the case $\alpha = 30^\circ$ regular reflection occurs, while for $\alpha = 90^\circ$ and a Mach disk is formed. The relevant fluid dynamic features in the latter case are the rarefactions at the

orifice, the so-called barrel shocks, the Mach disk shock, and the shocks radiating outward from the Mach disk triple point.

Additional results with different vent conditions and crater geometry, together with results with adaptive mesh refinement and in three-dimensions can be found in [15].

Acknowledgments

This work was supported in part by DOE grant DE-FG03-96ER25292 and NSF grant DMS-0106511. The authors thank A. Neri and T. Esposti Ongaro of the Istituto Nazionale di Geofisica e Vulcanologia (Pisa, Italy) for their invaluable suggestions in the development of this work.

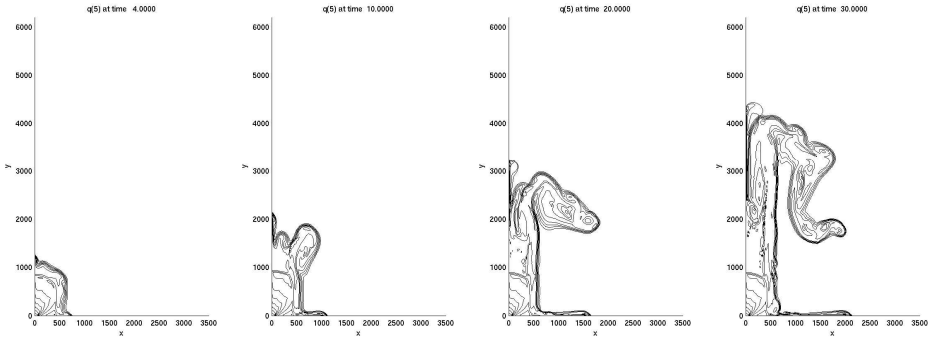

FIGURE 1. $\alpha = 90°$. Dust density contours at $t = 4$, 10, 20, 30 s.

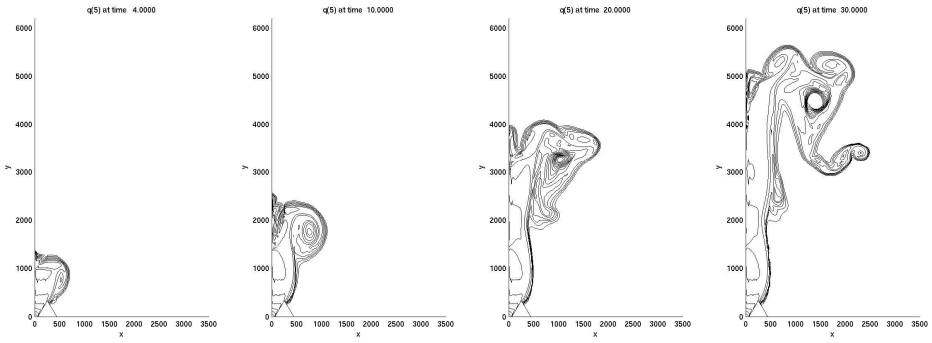

FIGURE 2. $\alpha = 30°$. Dust density contours at $t = 4$, 10, 20, 30 s.

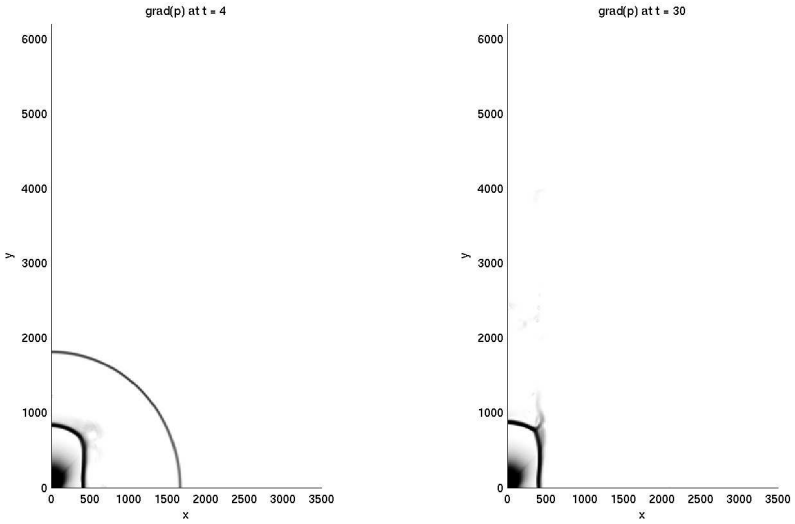

FIGURE 3. $\alpha = 90°$. Pressure gradient at $t = 4$, 30 s.

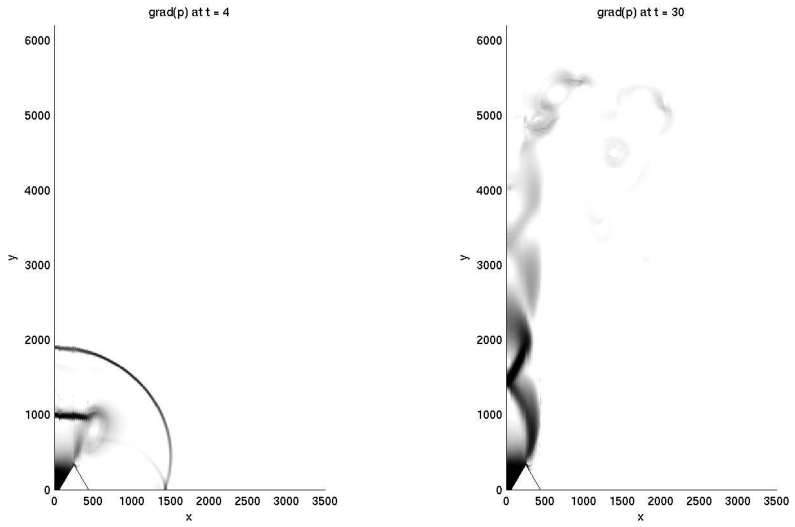

FIGURE 4. $\alpha = 30°$. Pressure gradient at $t = 4$, 30 s.

References

[1] D. S. BALE, R. J. LEVEQUE, S. MITRAN, AND J. A. ROSSMANITH, A wave-propagation method for conservation laws with spatially varying flux functions, *SIAM J. Sci. Comput.*, **24** (2002), 955–978.

[2] F. Dobran, A. Neri and G. Macedonio, Numerical Simulation of Collapsing Volcanic Columns, *J. Geophys. Res.*, **98** (1993), 4231–4259.
[3] F. H. Harlow and A. A. Amsden, Numerical calculation of Multiphase Fluid Flow, *J. Comput. Phys.*, **17** (1975), 19–52.
[4] S. W. Kieffer and B. Sturtevant, Laboratory Studies of Volcanic Jets, *J. Geophys. Res.*, **89**, Vol. B10 (1984), 8253–8268.
[5] R. J. LeVeque, Wave Propagation Algorithms for Multidimensional Hyperbolic Systems, *J. Comput. Phys.*, **131** (1997), 327–353.
[6] R. J. LeVeque, clawpack software, available at `http://www.amath.washington.edu/~claw`.
[7] R. J. LeVeque, The dynamics of pressureless dust clouds and delta waves, *J. Hyperbolic Diff. Eq.*, **1** (2004), 315-327.
[8] R. J. LeVeque and M. Pelanti, A Class of Approximate Riemann Solvers and Their Relation to Relaxation Schemes, *J. Comput. Phys.*, **172** (2001), 572–591.
[9] R. J. LeVeque and M. Pelanti, High-resolution finite volume methods for dusty gas jets and plumes, submitted to SIAM J. Sci. Comput. (2005).
[10] A. Neri and F. Dobran, Influence of eruption parameters on the thermofluid dynamics of collapsing volcanic columns, *J. Geophys. Res.*, **99** (1994), 11833–11857.
[11] A. Neri and G. Macedonio, D. Gidaspow, and T. Esposti Ongaro, Multiparticle simulation of collapsing volcanic columns and pyroclastic flows, *J. Geophys. Res.*, **108** No. B4 (2003), 1–22.
[12] A. Neri, P. Papale and G. Macedonio, The role of magma composition and water content in explosive eruptions, 2. Pyroclastic dispersion dynamics, *J. Volcanol. Geotherm. Res.*, **87** (1998), 95-115.
[13] T. Esposti Ongaro and A. Neri, Flow Patterns of Overpressured Volcanic Jets, European Geophysical Society, XXIV General Assembly, The Hague, 19-23 April 1999.
[14] P. Papale, A. Neri and G. Macedonio, The role of magma composition and water content in explosive eruptions, 1. Conduit ascent dynamics, *J. Volcanol. Geotherm. Res.*, **87** (1998), 75–93.
[15] M. Pelanti, Wave Propagation Algorithms for Multicomponemt Compressible Flows with Applications to Volcanic Jets, *Ph. D. Thesis*, University of Washington, Seattle (2005).
[16] P. L. Roe, Approximate Riemann Solvers, Parameter Vectors and Difference Schemes, *J. Comput. Phys.*, **43** (1981), 357–372.
[17] T. Saito, Numerical Analysis of Dusty-Gas Flow, *J. Comput. Phys.*, **176** (2002), 129–144.
[18] L. Sainsaulieu, Finite volume approximation of two-phase fluid flows based on an approximate Roe-type Riemann solver, *J. Comput. Phys.*, **121** (1995), 1-28.
[19] G. A. Valentine and K. H. Wohletz, Numerical Models of Plinian Eruption columns and Pyroclastic Flows, *J. Geophys. Res.*, **94** (1989), 1867–1887.
[20] K. H. Wohletz, T. R. McGetchin, M. T. Sanford II, and E. M. Jones, Hydrodynamic forming of caldera-forming eruptions: numerical models, *J. Geophys. Res.*, **89** (1984), 8269–8285.

Department of Applied Mathematics
University of Washington, Box 352420, Seattle, WA 98195-2420
E-mail address: `pelanti@amath.washington.edu`

Department of Applied Mathematics and Department of Mathematics
University of Washington, Box 352420, Seattle, WA 98195-2420
E-mail address: `rjl@amath.washington.edu`